



OPEN Combination of gut microbiota, proinflammatory cytokine, and ^{18}F -FDG PET as potential indicators for predicting breast cancer recurrence

Jeongshin An^{1,4}, Bom Sahn Kim²✉ & Hai-Jeon Yoon³✉

Breast cancer occurs at a younger age compared to western countries in South Korea. Despite advancements in treatment methods such as targeted therapy and immunotherapy, the increasing number of patients underscores the importance of improving disease-free survival (DFS). In this study, we evaluated the associations between gut microbiota composition, inflammatory cytokine levels, and breast cancer recurrence in preoperative patients. Additionally, we developed a composite prognostic index by integrating these factors with PET/CT indices and clinical prognostic factors. This study showed that *Prevotella* abundance was significantly higher in the DFS group than in the recurrence group, and higher *Prevotella* abundance was associated with lower levels of the inflammatory cytokine IL-1 β . Survival analysis revealed that patients with low *Prevotella* abundance and high IL-1 β levels had a higher risk of breast cancer recurrence. PET markers, such as $\text{SUV}_{\text{tumor}}$, SUV_{VAT} , and $\text{SUV}_{\text{spleen}}$, were also found to be significant prognostic indicators, with lower values associated with better survival outcomes. An integrated predictive model combining gut microbiota composition, cytokine levels, PET indices, and clinical factors demonstrated superior accuracy (AUC: 0.9025) in predicting breast cancer recurrence compared to individual components.

Keywords ^{18}F -FDG PET, Gut microbiota, Tumor uptake, Spleen uptake, Pro-inflammatory cytokine, Breast cancer, Recurrence

Breast cancer remains the most prevalent cancer among women worldwide, with 2.26 million new cases reported in 2020¹. Despite advancements in early detection through improved imaging techniques and diagnostic biomarkers, tumor recurrence and metastases continue to significantly impact both incidence and mortality rates among breast cancer patients following standard treatments².

Currently used tumor markers for breast cancer diagnosis and recurrence monitoring, carcinoembryonic antigen (CEA) and carcinoma antigen 15–3 (CA15–3), have limitations³. CEA has poor specificity for breast cancer, while CA15–3 has a positivity rate of 30–50% in patients with breast cancer⁴. These shortcomings highlight the need for the development of novel biomarkers to predict breast cancer recurrence and disease-free survival (DFS).

There is increasing interest in the potential causal relationship between the gut microbiota and various types of cancer, including breast cancer^{5–8}. There is accumulating evidence that the influence of gut microbiota is associated with the development and progression of not only gastrointestinal cancer but also breast cancer. Microbial dysbiosis can lead to intestinal hyperpermeability, chronic inflammation, and ultimately contribute to carcinogenesis^{5,9}.

¹Institute of Convergence Medicine Research, Ewha Womans University Mokdong Hospital, Ewha Womans University College of Medicine, 1071 Anyangcheon-ro, Yangcheon-gu, Seoul 07985, Republic of Korea. ²Department of Nuclear Medicine, Ewha Womans University Seoul Hospital, Ewha Womans University College of Medicine, 260 Gonghang-daero, Gangseo-gu, Seoul 07804, Republic of Korea. ³Department of Nuclear Medicine, Ewha Womans University Mokdong Hospital, Ewha Womans University College of Medicine, 1071 Anyangcheon-ro, Yangcheon-gu, Seoul 07985, Republic of Korea. ⁴Department of Surgery, Ewha Womans University Mokdong Hospital, Ewha Womans University School of Medicine, 1071 Anyangcheon-ro, Yangcheon-gu, Seoul 07985, Republic of Korea. ✉email: kbomsahn@ewha.ac.kr; haijeon.yoon@ewha.ac.kr

Chronic inflammation, especially that induced by obesity, is known to play a key role in the pathogenesis of breast cancer¹⁰. When obesity induces inflammation within breast adipose tissue, a characteristic process occurs in which macrophages accumulate around adipocytes that secrete inflammatory cytokines, leading to apoptosis and necrosis of adipocytes. This creates a microenvironment that favors mutation, cancer cell proliferation, and highly metastatic tumor formation.

F-18 fluorodeoxyglucose (FDG) positron-emission tomography (PET) has emerged as a valuable tool in oncology, not only for evaluating tumor metabolism but also for assessing systemic inflammation. In breast cancer, PET contributes to accurate staging and provides prognostic information. The standardized uptake value (SUV) of tumors, as well as uptake in the spleen and adipose tissue, have been reported as strong prognostic indicators^{11–14}.

Despite accumulating evidence supporting the involvement of gut microbiota and inflammatory responses involved in the initiation and progression of breast cancer, how specific microbiome profiles may contribute to breast cancer recurrence through inflammation-related mechanisms remains largely unexplored. Therefore, we aimed to investigate the association between gut microbiota and inflammatory cytokines in preoperative breast cancer patients and assessed the prognostic value of gut microbiome dysbiosis and inflammatory cytokines for breast cancer recurrence. In addition, a composite prognostic index by combining established FDG PET and clinical prognostic factors with gut microbiota and blood cytokine levels was developed.

Results

Patient characteristics

Patient characteristics are summarized in Table 1. The study involved 113 breast cancer patients with an average age of 50 years. The majority of patients had breast tumors 2 cm or smaller in size. Regarding lymph node status, 66.4% were negative for metastasis, while 32.7% were positive. The most prevalent breast cancer subtype was the luminal subtype (78.8%), followed by HER2 subtype (9.7%) and triple-negative breast cancer (TNBC) subtype at 8.8%. The average levels of inflammatory markers were 1.26 pg/mL for IL-1 β and 3.6 mg/dL for CRP. After a 7 to 8 year follow-up period, 101 patients (89.4%) remained DFS, while 12 patients (10.6%) experienced breast cancer recurrence.

Comparison of richness and diversity in gut microbiota

The overall gut microbial compositions of patients with breast cancer were shown at different taxonomic levels. Predominantly, Phyla Firmicutes and Bacteroidetes constituted most of the stool microbiome, collectively accounting for approximately 92.9% in DFS and 88.9% in recurrence group (Fig. 1). In Fig. 1A, alpha diversity is shown using the ACE index, and in Fig. 1B, beta diversity is represented by PCoA. In Supplementary Fig. 1, species richness is also demonstrated using the Jackknife and Chao1 indices, and diversity is measured by the Shannon, Simpson, and number of species indices. Figure 1C shows microbiome differences at the phylum level, while Fig. 1D presents these differences at the genus level. The microbiome differences from phylum to species levels can be found in Supplementary Fig. 2. Following these, Phyla Proteobacteria and Acinetobacteria were prevalent, together comprising up to 6% in non-recurrence and 7.9% in recurrence group of the total microbiome (Fig. 1C). Upon further stratification into DFS and recurrence groups, Firmicutes were found to be more abundant in the recurrence group. Conversely, the genus *Prevotella* was significantly more prevalent in the DFS group (Fig. 1D).

Changes in gut microbial compositions according to pro-inflammatory cytokine levels

The identification of microbiome biomarkers that distinguish between the DFS and recurrence groups was performed. Specific biomarkers for each group were determined using LefSe analysis (Fig. 2A). Analysis revealed significant differences in gut microbial composition between the DFS and the recurrence group, with *Prevotella* being notably abundant in the DFS group (Fig. 2A–B). Moreover, the proportion of *Prevotella* showed a gradual decreasing trend as the cancer stage progressed, with mean values of 9.4% in stage I, 8.0% in stage II, and 7.8% in stage III. Although this trend was not statistically significant, a decline was observed across stages. To further investigate the relationship between *Prevotella* abundance and cancer recurrence, we examined the correlation between blood cytokine levels and changes in *Prevotella* compositions. We determined an optimal cutoff value for IL-1 β , a key pro-inflammatory cytokine, using ROC curve analysis. Based on the ROC curve analysis of patient data according to their recurrence status, the optimal cutoff value for IL-1 β was established at 0.44. Using this cutoff, we divided breast cancer patients into two groups: low IL-1 β (<0.4415) and high IL-1 β (\geq 0.4415). Subsequent microbiome analysis of these groups revealed that patients in the low IL-1 β group had a statistically significant higher abundance of *Prevotella* compared to the high IL-1 β group (Fig. 2C). Although no statistically significant difference was found between patients grouped by CRP levels (<0.5 and \geq 0.5), there was a noticeable trend where the group with low CRP levels tended to have a higher abundance of *Prevotella*, as illustrated in Fig. 2D.

Observing that *Prevotella* differed between the low IL-1 β group and the high IL-1 β group, we compared the microbiome differences between these groups (Fig. 3). Each group was compared at the phylum, class, order, and genus levels, and bacteria were listed in order of abundance (Fig. 3A). For bacteria that were not clearly identified, they were designated by their higher taxon. Phylum Firmicutes, order Clostridiales, class Clostridia and class Verrucomicrobiae, genus *Blautia*, and genus *Akkermansia* were predominant in the high IL-1 β group (Fig. 3B). Including genus *Prevotella*, phylum Bacteroidetes, class Bacteroidia, order Bacteroidales, and species *Bacteroides stercoris* were predominant in the low IL-1 β group (Fig. 3C). We confirmed the relationship between *Prevotella* and breast cancer recurrence and found that IL-1 β might be involved. Additionally, we observed differences in the microbiota depending on IL-1 β levels, suggesting that IL-1 β may be involved in prognosis. Figure 3.

Characteristics	Patients with breast cancer
Female	113 (100%)
Age (mean \pm SD)	49.6 (\pm 9.3)
Menopausal status	
Premenopause	58 (51.3%)
Postmenopause	49 (43.4%)
Unknown	6 (5.3%)
BMI (kg/m ²)	
<18.5	5 (4.4%)
18.5–24.9	74 (65.5%)
25–29.9	28 (24.8%)
>30	6 (5.3%)
Operation	
Breast conserving surgery	85 (75.2%)
Modified radical mastectomy	27 (23.9%)
Unknown	1 (0.9%)
Tumor size	
pTis	1 (0.9%)
pT1	67 (59.3%)
pT2	38 (33.6%)
pT3	5 (4.4%)
pT4	1 (0.9%)
Unknown	1 (0.9%)
Nodal status	
pN0	75 (66.4%)
pN1	31 (27.4%)
pN2	5 (4.4%)
pN3	1 (0.9%)
Unknown	1 (0.9%)
Subtype	
Luminal A	29 (25.7%)
Luminal B	60 (53.1%)
HER2	11 (9.7%)
TNBC	10 (8.8%)
Unknown	3 (2.7%)
Serum tests (mean \pm SD)	
IL-1 β (pg/mL)	1.26 (\pm 4.0)
CRP (mg/dL)	3.6 (\pm 5.0)

Table 1. Characteristics of the patients.

***Prevotella* abundance and IL-1 β cytokine level in relation to breast cancer recurrence**

We analyzed the association between breast cancer recurrence and *Prevotella* abundance and IL-1 β cytokine levels. ROC curve analysis determined optimal cut-off points for *Prevotella* abundance and IL-1 β showing a threshold of 0.0130 and 0.4415, respectively. Survival probability curves demonstrated statistically significant differences between groups. Patients with higher *Prevotella* abundance showed better survival probability over time compared to those with lower levels, with $p=0.032$ (Fig. 4A). Conversely, patients with lower IL-1 β levels exhibited better survival probability than those with higher levels, $p=0.047$ (Fig. 4B). In multivariate Cox regression analysis adjusted for age and BMI, *Prevotella* abundance remained a significant predictor ($p=0.044$), while IL-1 β was marginally significant ($p=0.050$).

PET and clinical indices in relation to breast cancer recurrence

The analysis of PET and clinical indices revealed significant associations with breast cancer recurrence. ROC curve analysis determined optimal cut-off points for PET indices including SUV_{tumor} (threshold: 5.6850), SUV_{VAT} (threshold: 0.5050), and SUV_{spleen} (threshold: 2.1750). Survival probability curves demonstrated statistically significant differences between groups for all examined indices. Patients with lower SUV_{tumor} values showed significantly better survival probability over time compared to those with higher values, with $p=0.0054$ (Fig. 5A). Similar patterns were observed for SUV_{VAT} ($p=0.016$) and SUV_{spleen} ($p=0.0024$), with lower values associated with better outcomes (Fig. 5B–C). Of clinical indices, TNM staging showed a significant impact

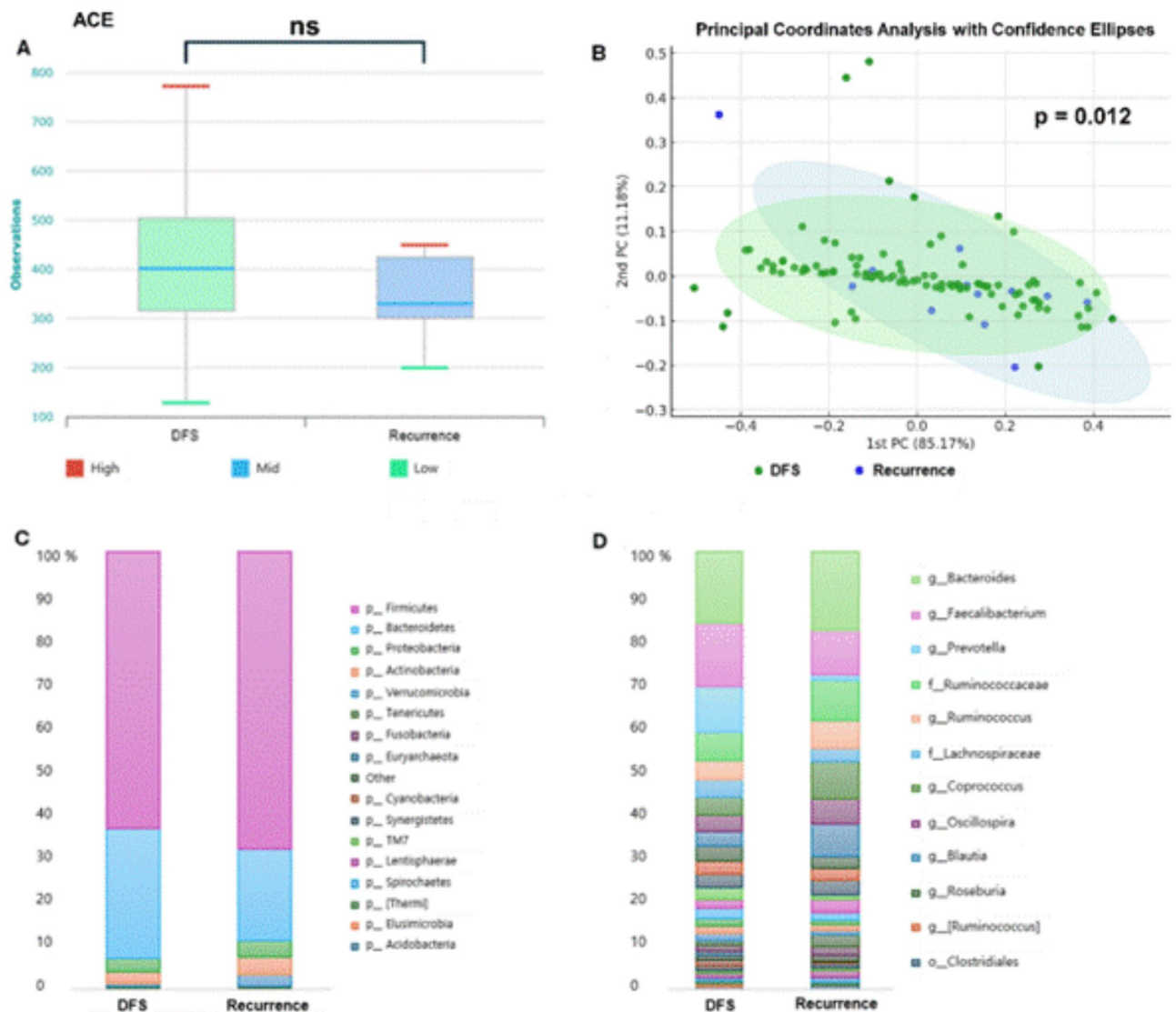


Fig. 1. Comparison of alpha and beta diversity and microbiome differences between DFS and Recurrence group in patients with breast cancer. **A.** The ACE (Abundance-based Coverage Estimator) index shows the alpha diversity at species level. **B.** PCoA (Principal Coordinates Analysis) with 65% confidence ellipses displays beta diversity at the phylum level, with blue dots representing the recurrent group and green dots representing the DFS group ($p=0.012$). **C.** Differences between the DFS and recurrence groups at the phylum level, and **D.** the genus level. The bacterial composition of each group was determined using a selection criterion of a P-value below 0.05.

on survival ($p=0.033$), with lower stages having better prognosis. Breast cancer subtypes also demonstrated significant differences in survival ($p=0.011$), with poorer outcomes especially in TNBC subtypes (Fig. 6).

The predictive performance of the combined gut microbiota, pro-inflammatory cytokine, PET, and clinical indices for breast cancer recurrence

Using the ROC analysis approach, we evaluated the performance of various factors in identifying patients with DFS and recurrence. We categorized these factors into four panels.

Panel 1 combined *Prevotella* abundance (AUC 0.5774, 95% CI: 0.4709–0.7085) and IL-1 β cytokine level (AUC 0.6153, 95% CI: 0.4502–0.7753), resulting in an AUC of 0.6035 (95% CI: 0.4667–0.7635).

Panel 2 analyzed PET indices: SUV_{tumor} (AUC 0.672, 95% CI: 0.5294–0.7812), SUV_{VAT} (AUC 0.6192, 95% CI: 0.4161–0.7942), and SUV_{spleen} (AUC 0.6815, 95% CI: 0.5393–0.8402). The combined PET indices showed an AUC of 0.6941 (95% CI: 0.5449–0.8126).

Panel 3 evaluated clinical indices: cancer subtype (AUC 0.6039, 95% CI: 0.4109–0.7923) and pathologic TNM staging (AUC 0.7421, 95% CI: 0.5987–0.878). Their combination achieved an AUC of 0.8139 (95% CI: 0.713–0.9538).

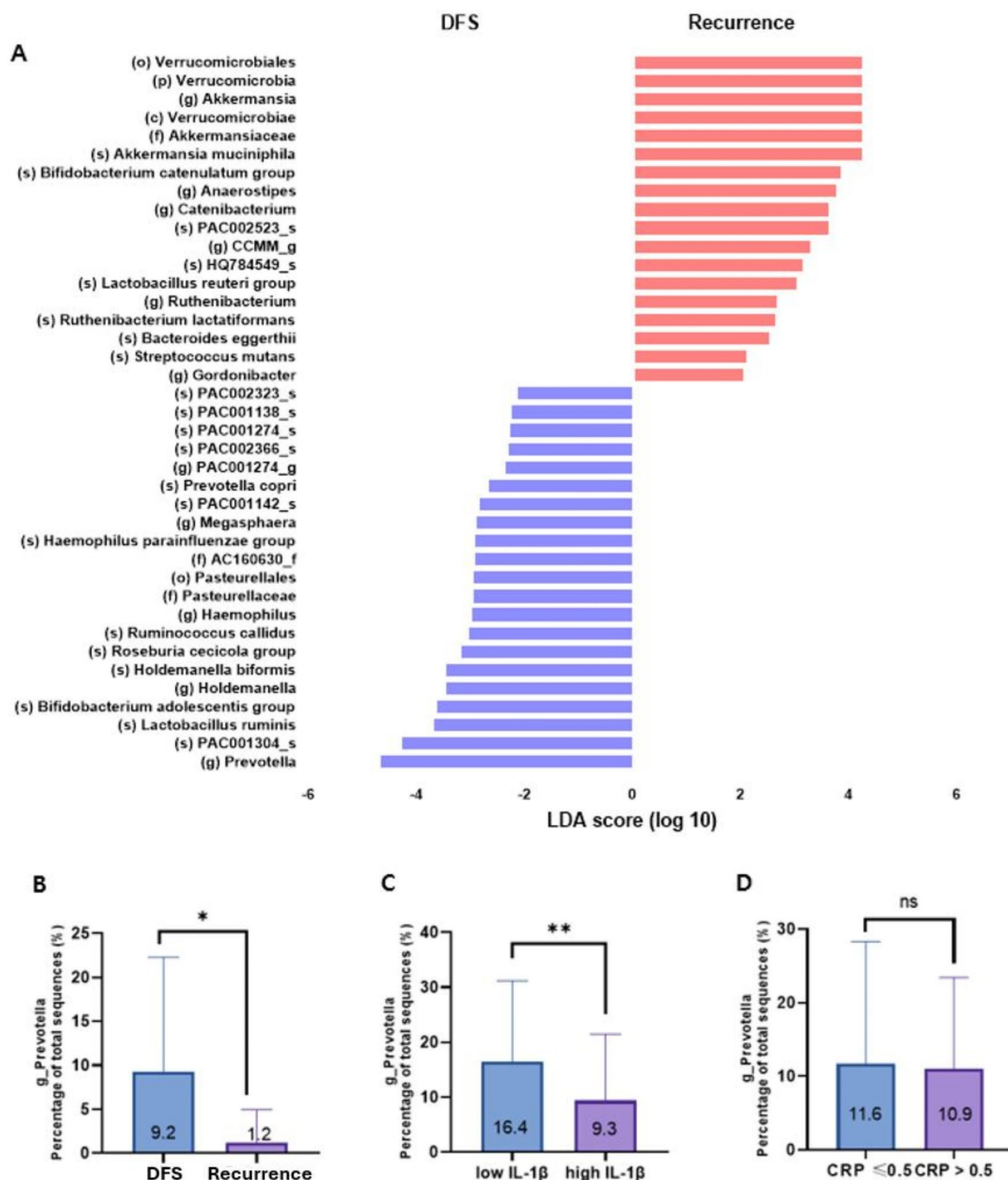
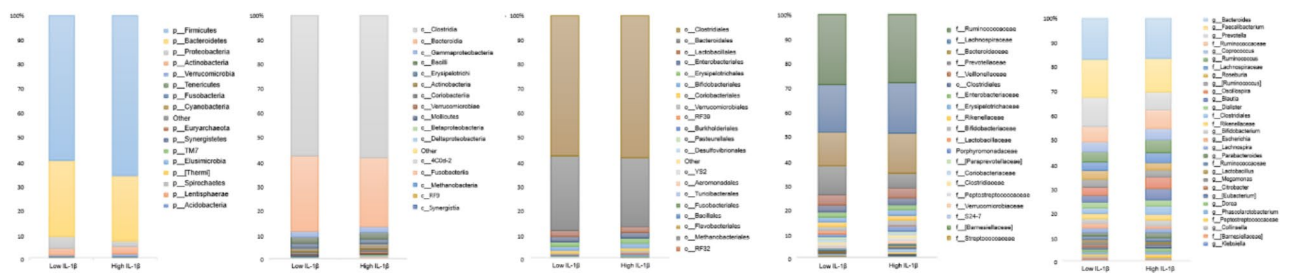


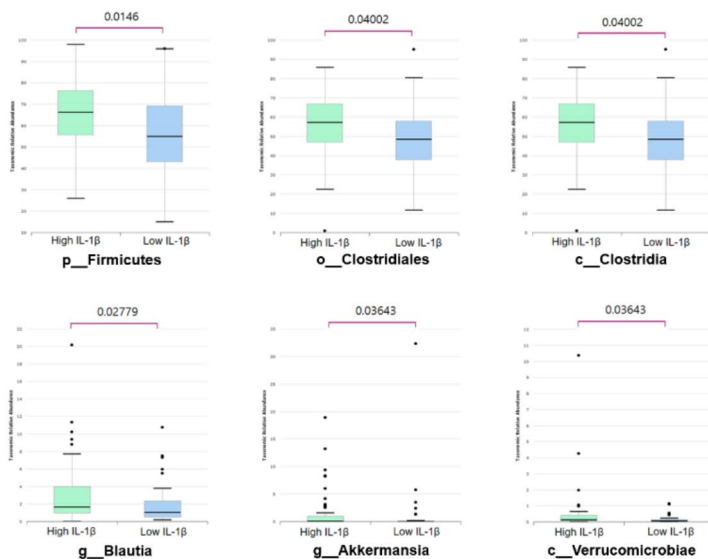
Fig. 2. The process of identifying microbiome biomarkers that differ between the DFS and recurrence groups. **A.** Identification of specific biomarkers for DFS and recurrence groups through LefSe analysis. **B.** *Prevotella* abundance differs between the DFS and recurrence groups. **C.** Comparison of *Prevotella* abundance between groups with high and low IL-1 β levels. **D.** Difference in *Prevotella* abundance between groups with high and low CRP levels.

Finally, Panel 4 integrated Panels 1, 2, and 3 into a comprehensive model, achieving the highest predictive performance with an AUC of 0.9025 (95% CI: 0.8046–0.9564). This significant improvement over Panel 1 and Panel 2 ($p < 0.001$ and $p = 0.032$, by Bootstrap) suggests that the combination of plasma markers, gut microbiota, PET, and clinical indices provides optimal predictive performance for recurrence. However, the lack of significant

A



B



C

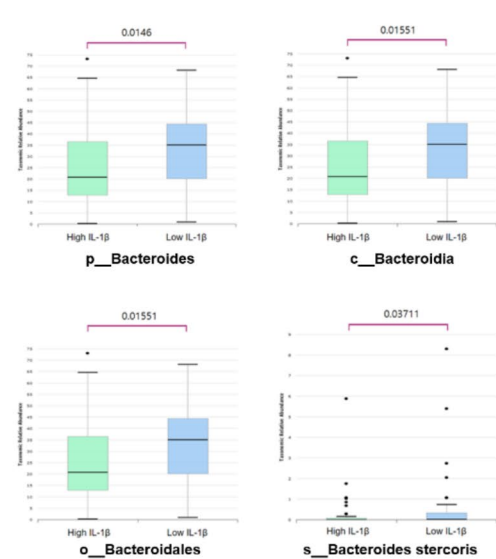


Fig. 3. The overall gut microbial compositions of the high and low IL-1 β groups are shown at different taxonomic levels. **A.** Microbiome differences between high and low IL-1 β groups, **B.** Abundant microbiome in high IL-1 β levels, **C.** Abundant microbiome in low IL-1 β levels.

improvement over Panel 3 ($p=0.204$, by Bootstrap) indicates that clinical indices alone may already offer strong predictive power. The results of all analyses are summarized in Table 2; Fig. 7.

Discussion

The age of breast cancer onset in Korea is highest in the 40–49 age group, which is younger than in Western countries¹⁵. In addition, the extension of survival time due to the development of treatment methods including targeted therapy and immunotherapy makes the achievement of disease-free survival (DFS) more important. In this study, we evaluated the associations between gut microbiota composition and inflammatory cytokine levels in preoperative breast cancer patients, explored the prognostic value for breast cancer recurrence, and developed a composite prognostic index by combining these factors with established FDG PET indices and clinical prognostic factors.

As a result, we found that *Prevotella* abundance was significantly higher in the DFS group than in the recurrence group, and that higher *Prevotella* abundance was associated with lower IL-1 β levels. Such a negative correlation between *Prevotella* abundance and IL-1 β pro-inflammatory cytokine further supports the idea that this genus may contribute to a favorable inflammatory profile. Survival analysis revealed that the low *Prevotella* abundance group and the high IL-1 β group had a poor prognosis for breast cancer recurrence. These findings indicate the potential protective role and prognostic value of gut microbiome composition and inflammatory cytokine levels in breast cancer.

Prevotella is known to be involved in the production of propionic acid, a short-chain fatty acid. The metabolic products of *Prevotella* are thought to participate in lowering serum cholesterol levels, reducing hepatic fat production, and alleviating adipose tissue accumulation¹⁶. The abundance of *Prevotella* in the gut microbiota appears to be correlated with dietary patterns rich in fiber and complex carbohydrates in rural and non-Western populations. This relationship indicates a possible protective role of *Prevotella* in maintaining optimal gut mucosal integrity. Interestingly, some researchers have reported that high abundance of *Prevotella* is associated with a lower incidence of colorectal cancer, which shares obesity as a risk factor with breast cancer,

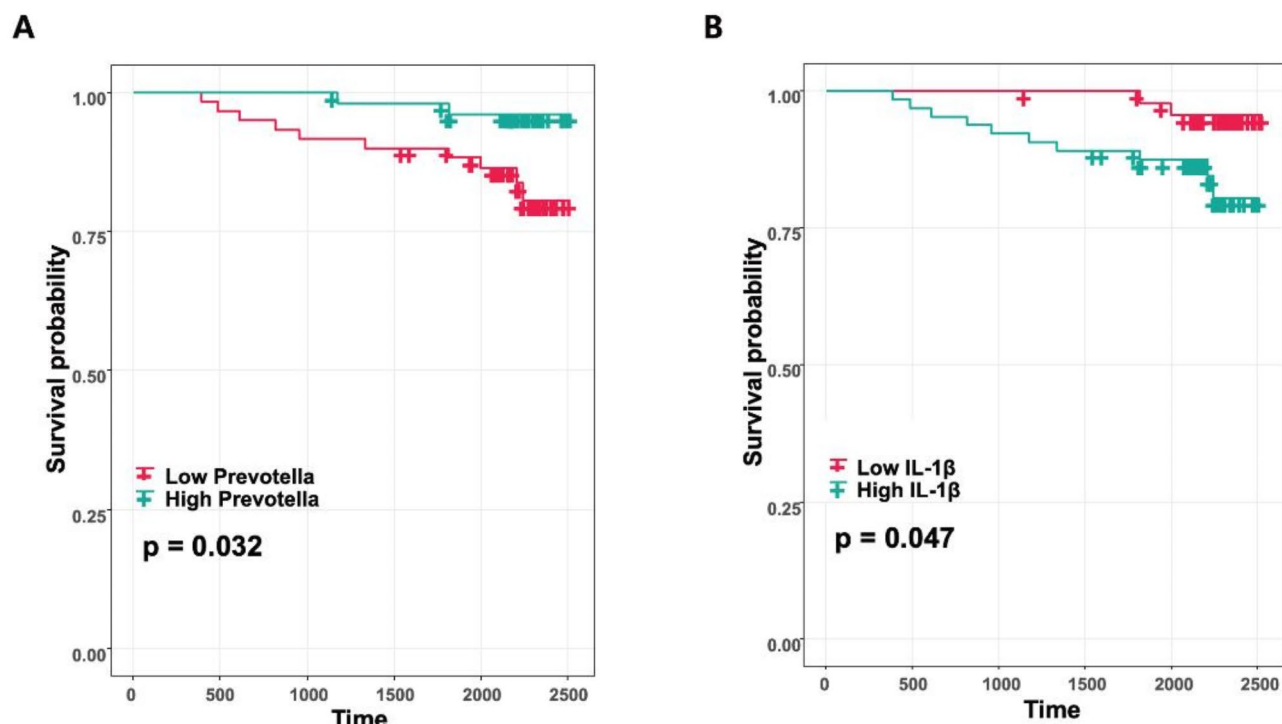


Fig. 4. Kaplan-Meier survival curves showing the association between breast cancer recurrence, *Prevotella* abundance, and IL-1 β levels. **A.** Survival probability curves for breast cancer recurrence based on *Prevotella* abundance, with patients stratified into high (green) and low (red) groups (cut-off: 0.0130, $p = 0.032$). **B.** Survival probability curves for breast cancer recurrence based on IL-1 β levels, with patients stratified into high (green) and low (red) groups (cut-off: 0.4415, $p = 0.047$).

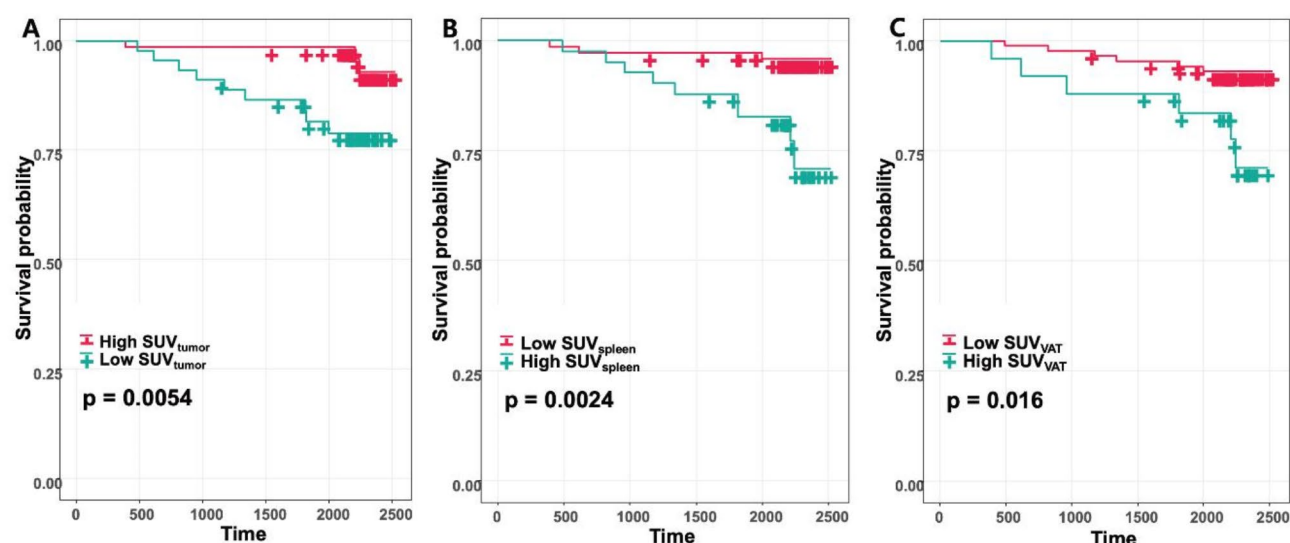


Fig. 5. Kaplan-Meier survival curves showing the association between breast cancer recurrence and PET indices. **A.** Survival probability curves based on SUV_{tumor}, with patients stratified into high (green) and low (red) groups (cut-off: 5.6850, $p = 0.0054$). **B.** Survival probability curves based on SUV_{spleen}, with patients stratified into high (green) and low (red) groups (cut-off: 2.1750, $p = 0.0024$). **C.** Survival probability curves based on SUV_{VAT}, with patients stratified into high (green) and low (red) groups (cut-off: 0.5050, $p = 0.016$).

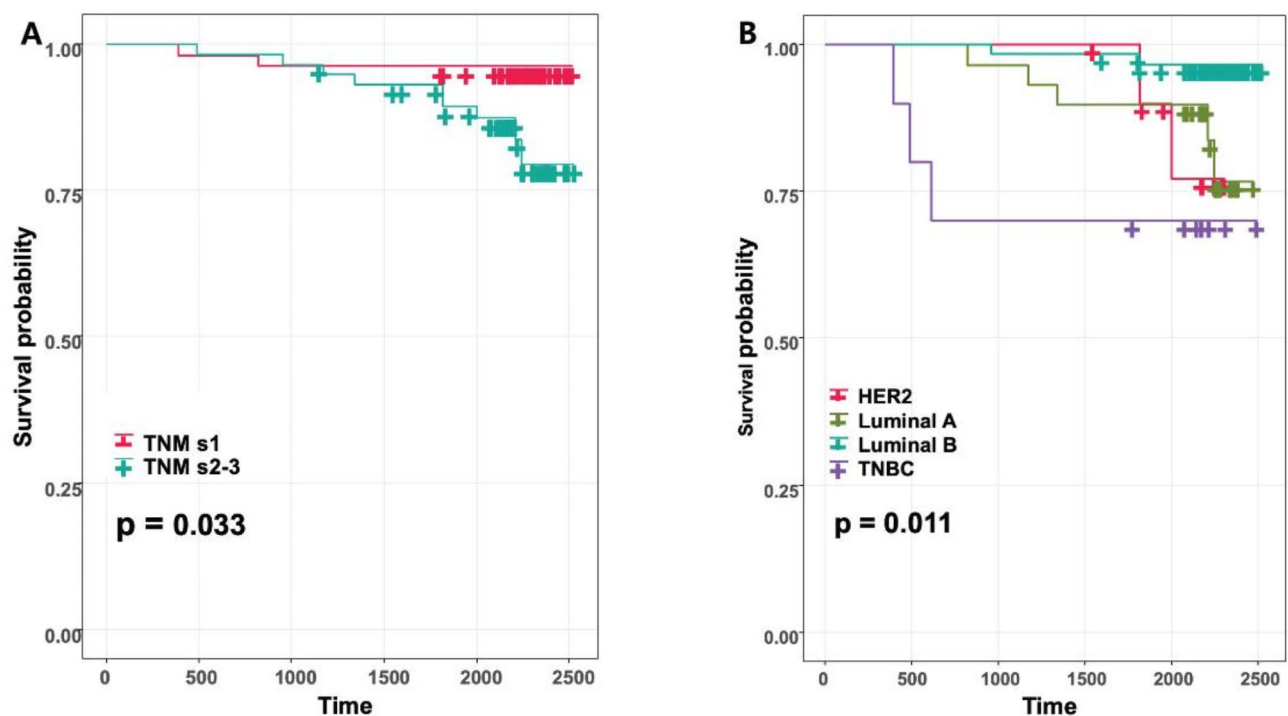


Fig. 6. Kaplan-Meier survival curves showing the association between breast cancer recurrence and clinical indices. **A.** Survival probability curves based on TNM staging, with patients stratified into s1 (red) and s2-3 (green) groups ($p = 0.033$). **B.** Survival probability curves based on breast cancer subtypes: HER2, Luminal A, Luminal B, and TNBC ($p = 0.011$).

	AUC	95% LCI	95% UCI	Sensitivity (%)	Specificity (%)	Accuracy (%)	ppv (%)	npv (%)
In vitro indices								
<i>Prevotella</i>	0.5417	0.3571	0.6881	81.82	47.92	51.4	15.25	95.83
IL-1 β	0.6264	0.4558	0.7948	81.82	48.96	52.34	15.52	95.92
Panel 1	0.5758	0.3972	0.7557	81.82	48.96	52.34	15.52	95.92
PET indices								
SUV _{tumor}	0.6591	0.5267	0.781	72.73	64.58	65.42	19.05	95.38
SUV _{VAT}	0.6027	0.4034	0.7751	45.45	85.42	81.31	26.32	93.18
SUV _{spleen}	0.6809	0.4832	0.8419	81.82	66.67	68.22	21.95	96.97
Panel 2	0.6941	0.5313	0.8197	81.82	63.54	65.42	20.45	96.83
Clinical indices								
Subtype	0.6039	0.3962	0.783	63.64	66.33	66.06	17.5	94.2
Stage	0.7421	0.5987	0.878	45.45	91.84	87.16	38.46	93.75
Panel 3	0.8139	0.713	0.9538	63.64	89.58	86.92	41.18	95.56
Combined model								
Panel 4	0.9025	0.8046	0.9564	100	71.88	74.77	28.95	100

Table 2. Predictive performance of in vitro, PET, and clinical indices and their combinations for breast Cancer recurrence.

and a better prognosis in colorectal cancer patients^{17,18}. On the other hand, there exist studies reporting that specific *Prevotella* strains can promote chronic inflammatory diseases such as periodontitis, rheumatoid arthritis, bacterial vaginosis, and HIV infection¹⁹. This suggests that the interaction between microbes and the host immune system may vary depending on the specific strain and environmental context.

Patients in the low IL-1 β group showed significantly higher *Prevotella* abundance compared to patients in the high IL-1 β group, whereas a similar trend toward increased *Prevotella* abundance was observed in patients with low CRP levels, although this association did not reach statistical significance. The stronger association of *Prevotella* abundance with IL-1 β than with CRP is particularly noteworthy in the context of breast cancer. Unlike diseases where systemic inflammation is a primary concern, breast cancer patients may not exhibit dramatic

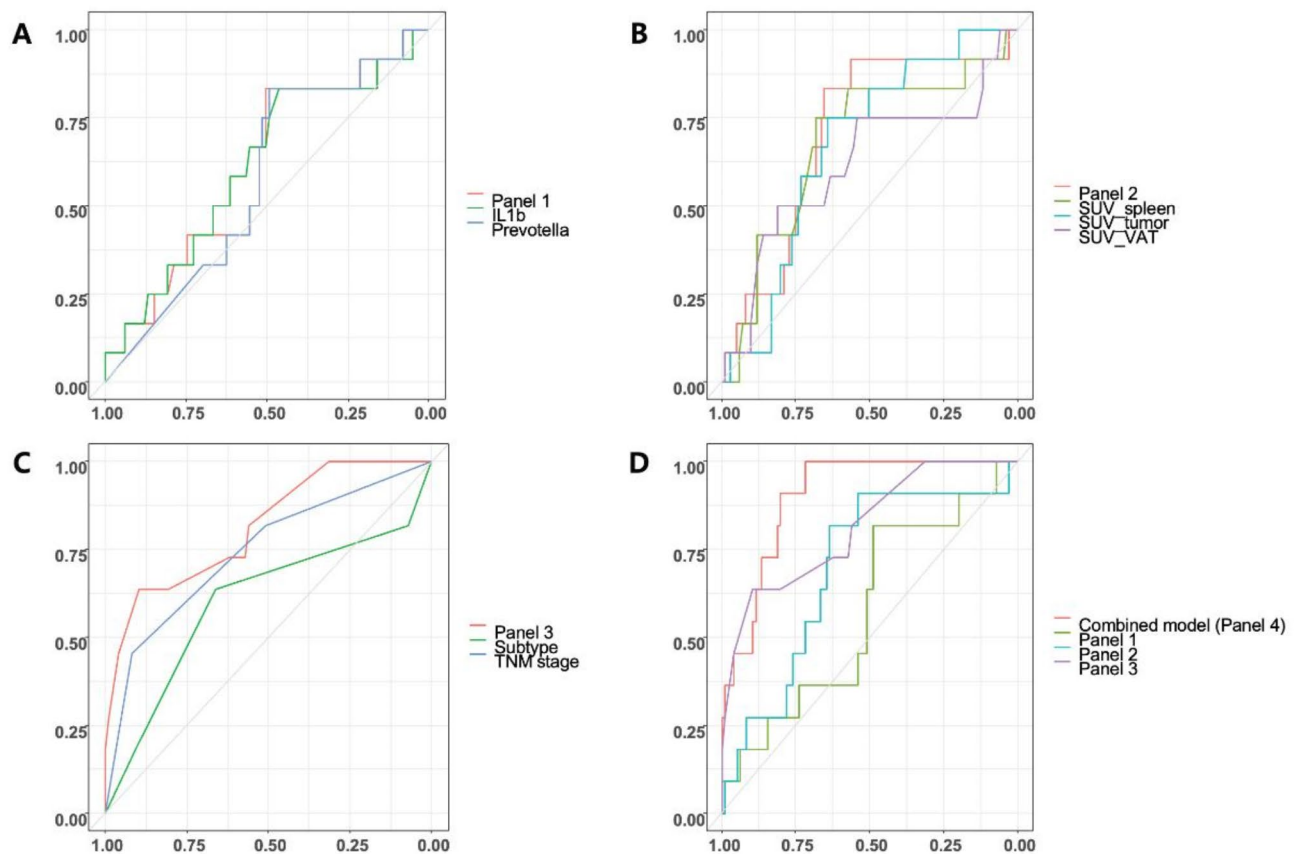


Fig. 7. ROC curves demonstrating the predictive performance of combined factors for breast cancer recurrence. **A.** In vitro indices: ROC curves for *Prevotella* abundance, IL-1 β cytokine level, and their combination, Panel (1) **B.** PET indices: ROC curves for SUV_{tumor} , SUV_{VAT} , SUV_{spleen} , and their combination, Panel (2) **C.** Clinical indices: ROC curves for cancer subtype, TNM stage, and their combination, Panel (3) **D.** Comparison of ROC curves for Panels 1–3 and the combined model, Panel 4.

changes in broad inflammatory markers such as CRP. In this regard, IL-1 β , a more specific inflammatory cytokine, may be considered a more sensitive indicator of the relationship between inflammation and gut microbiota composition²⁰. Furthermore, these results suggest that inflammatory responses contribute to the complex interplay between the gut microbiome and breast cancer.

Our study confirmed better prognosis in the group with lower values of SUV_{tumor} , SUV_{VAT} and SUV_{spleen} , which is consistent with previous studies. The prognostic significance of SUV_{tumor} in breast cancer has been well-documented. A meta-analysis by Lee et al. demonstrated that high SUV_{tumor} was associated with poor prognosis in breast cancer patients, with a pooled hazard ratio of 3.01 (95% CI: 1.83–4.97) for event-free survival²¹. The prognostic value of SUV_{spleen} and SUV_{VAT} as PET markers reflecting systemic inflammation in breast cancer has also been increasingly recognized. Kim et al. reported that high SUV_{VAT} was associated with poor recurrence-free survival with a hazard ratio of 2.754 (95% CI: 1.090–6.958)¹³. Bang et al. found that high SUV_{spleen} was an independent negative prognostic factor for DFS in breast cancer patients¹².

Finally, we developed a multi-modal predictive model by integrating gut microbiota, cytokine levels, PET indices, and traditional clinical factors (TNM staging and breast cancer subtypes). This integrated predictive model demonstrated superior predictive performance compared to models based on individual components in breast cancer prognosis assessment, achieving an AUC of 0.9025 (95% CI: 0.8046–0.9564). The success of this approach appears to reflect the pathophysiology of breast cancer as a complex multi-system disease influenced by various physiological and environmental factors.

In this study, we found that *Prevotella* abundance was significantly higher in the DFS group than in the recurrence group, and that high *Prevotella* abundance was associated with lower IL-1 β levels. In addition, we found that the group with low *Prevotella* abundance had an increased risk of breast cancer relapse compared to the group with high abundance, and the group with high IL-1 β levels had an increased risk of breast cancer recurrence compared to the group with low abundance. In terms of imaging biomarkers, the group with low values of PET markers (SUV_{tumor} , SUV_{VAT} and SUV_{spleen}) had better survival outcomes than the group with high values. Among clinical indicators, TNM stage and breast cancer subtype were significant prognostic factors, and among the subtypes, TNBC showed a poor prognosis. In particular, the integrated model combining gut microbiota composition, inflammatory cytokine levels, PET markers, and clinical factors showed superior accuracy in predicting recurrence compared to using individual markers alone. These results indicate the

potential of a multimodal approach to assess the risk of breast cancer relapse and tailor personalized treatment strategies.

Our study has several limitations. First, it is a retrospective, single-center study with a small sample size. Moreover, since we included only patients who underwent preoperative PET/CT examinations, there may be selection bias affecting patient distribution, particularly in terms of breast cancer subtypes. Larger prospective multi-center studies are needed to validate our integrated predictive model across diverse populations and clinical settings. Second, while we have identified associations between gut microbiota, systemic inflammation, and breast cancer progression, the underlying mechanisms remain unveiled. Further investigations using *in vitro* and *in vivo* studies are necessary to elucidate the mechanistic links between gut microbiota, systemic inflammation, and breast cancer progression. Lastly, we did not consider the costs associated with PET imaging and microbiome analysis. A cost-effectiveness analysis would be beneficial in determining the feasibility of implementing this integrated approach in routine clinical practice.

Materials and methods

Subjects

This study recruited participants from patients undergoing PET/CT for initial breast cancer staging. Eligible participants met the following inclusion criteria: (1) Patients with no history of taking lipid-lowering drugs or probiotics within four weeks prior to enrollment, as these medications can influence gut microbiota; (2) Patients who had not undergone neoadjuvant chemotherapy before undergoing PET/CT; (3) Patients without concurrent inflammatory bowel disease, infectious colitis, etc., and (4) Patients who had not taken any antibiotics within six weeks prior to enrollment. From 121 female participants who underwent PET/CT between April 2016 and February 2017, 113 non-metastatic patients (stages 1 to 3) met all criteria and were included in the final analysis. Stool samples were collected for microbiome analysis, and blood samples were analyzed for Interleukin (IL)-1 β and C-reactive protein (CRP) levels. The study protocol was approved by the Institutional Review Board of Ewha University Medical Center (2016-01-017-002), and informed consent was obtained from all study participants. The study was conducted in full compliance with institutional and governmental guidelines for research involving human subjects. Patients were followed for 7 to 8 years until 2023 and categorized based on the recurrence development.

Clinicopathological and survival data

Clinicopathological data were retrieved from electronic medical records, encompassing information such as age at initial diagnosis, gender, menopausal status, and body mass index (BMI), defined as the ratio of body weight in kilograms to the square of height in meters. Pathological data encompassed pathologic stages (pT, pN), expression of estrogen receptor (ER), progesterone receptor (PR), and human epidermal growth factor receptor 2 (HER2). ER and PR positivity were determined based on both the percentage of positive cells (ranging from 0 to 5) and staining intensity (ranging from 0 to 3). A total score of 0–2 was considered negative for each hormone, while 3–8 was considered positive. HER2 status was categorized as negative for negative or 1+ immunohistochemistry results and positive for 3+ results. In cases with 2+ results, HER2 positivity was determined through fluorescence *in situ* hybridization (FISH) results.

Following curative surgery, adjuvant therapy was administered in accordance with pathologic staging and the clinical condition of the patients. Regular clinical follow-up involved physical examinations, blood tests, ultrasonography, chest X-rays, and bone scans every 3 to 6 months during the initial 2 years, followed by check-ups every 6 to 12 months thereafter. When the recurrence was suspected, additional procedures, including pathological confirmation or imaging studies, were conducted. For survival analysis, DFS was defined as the period between the date of the operation and the date of initial recurrence detection.

Stool DNA extraction and bacterial 16 S rRNA gene sequencing

Stool samples were frozen immediately after defecation at -20°C and placed in -70°C storage within 24 h. Stool DNA extraction was performed within one month with the MOBio PowerSoil[®] DNA Isolation Kit (MO BIO Laboratories, Carlsbad, CA), according to the manufacturer's instructions.

The methods used to bacterial 16S rRNA gene sequencing are detailed in our previous study²². Briefly, the universal primers 341F (5' TCG TCG GCA GCG TCA GAT GTG TAT AAG AGA CAG CCT ACG GGN GGC WGC AG 3') and 805R (5' GTC TCG TGG GCT CGG AGA TGT GTA TAA GAG ACA GGA CTA CHV GGG TAT CTA ATC C 3') were used to amplify the variable V3 and V4 regions of the 16 S rRNA gene. Each primer was modified to contain a unique 8 nt barcode index by adding Nextera XT DNA Library Preparation kit (Illumina, San Diego, CA). For PCR reactions, a 5 ng/ μL DNA template, 2 \times KAPA HiFi HotStart Ready Mix (KAPA Biosystems, Wilmington, MA), and 2 pmol of each primer were combined. The mixtures were incubated at 95°C for 3 min, followed by 25 cycles of 95°C for 30 s, 55°C for 30 s, and 72°C for 30 s. Samples were incubated for the final extension at 72°C for 5 min. Sequencing was performed on the Illumina MiSeq platform after PCR clean-up and indexing^{23,24}.

16 S rRNA gene-based microbiome taxonomic profiling and analysis

Microbiome taxonomic profiling (MTP) was performed using the EZBioCloud platform (<http://www.ezbiocloud.net/>, ChunLab Inc., Republic of Korea) with the PKSSU4.0 database version²⁵. The operational taxonomic unit (OUT) picking was conducted with UCLUST and CDHIT with a 97% similarity cutoff²⁶. Comparisons of the taxonomic composition according to levels of cytokines were performed using the comparative MTP analyzer implemented in EZBioCloud. Microbial richness and alpha-diversity were calculated and compared using the Wilcoxon rank-sum test. Beta-diversity was calculated and compared using pairwise Permutational Multivariate Analysis of Variance (PERMANOVA). These analyses were conducted using normalized data, considering

variations in gene copy number. Microbial richness was measured by ACE and Chao indices. Alpha-diversity was measured by Shannon and Simpson indices. Beta-diversity was measured by Bray-Curtis and generalized UniFrac distances. The identification of taxonomic biomarkers that exhibited differential abundance between the two groups was carried out using the linear discriminant analysis effect size (LEfSe) algorithm²⁷. Only taxa with LEfSe values > 2.0 were reported.

Serum cytokine analysis

Serum levels of IL-1 β were determined using an enzyme-linked immunosorbent assay (ELISA). Briefly, 96-well microtiter plates were first coated with the respective capture antibodies (human IL-1 β capture; R&D Systems) and incubated overnight at 4 °C. Following this, the plates were treated with a blocking buffer at room temperature. Test samples and standard recombinant proteins (human IL-1 β ; R&D Systems) were then added to each well, and this was succeeded by incubation with biotinylated detection antibodies (human IL-1 β detection; R&D Systems). After the incubation period, Streptavidin-Horseradish Peroxidase (Thermo Scientific) was introduced to the plates, followed by the TMB Substrate Solution (Thermo Scientific), with a reaction time of 30 min. The reaction was halted by adding a stopping solution, and the absorbance was quantified at 450 nm using a VersaMax microplate reader (Molecular Devices, LLC, USA).

¹⁸F-FDG PET/CT and image analysis

All patients were instructed to fast for at least six hours before intravenous FDG administration (5.18 MBq per kg) and to rest for the hour preceding the scan. Fasting blood glucose levels were measured and confirmed to be < 140 mg/dL prior to FDG administration. A low-dose CT scan without contrast was first acquired with a CARE Dose system, and then a PET scan was obtained from the skull base to the mid-thigh using a Siemens Biograph mCT with 128 CT slices (Siemens Medical Solutions, Erlangen, Germany). The spatial resolution of the PET scanner was 2.0 mm full width at half maximum (FWHM) in the trans-axial direction and 2.0 mm FWHM in the axial direction at the center of the PET. Three-dimensional emission mode was used for the acquisition parameters with 2 min scanning per bed position. PET images were reconstructed to 200 × 200 matrices and 3.4 mm × 3.4 mm pixel size, with 3.0 mm slice thickness, using a 3D-OSEM iterative algorithm (2 iterations and 21 subsets) with time of flight (TOF) and point spread function (PSF).

All PET/CT data were analyzed using a commercial software (Syngo.via VB60A, Siemens Medical Solutions, Erlangen, Germany) by two experienced nuclear physicians (HJY and BSK) and were averaged. The maximum standardized uptake value (SUV_{max}) of primary tumor (SUV_{tumor}) was measured by delineating a volume of interest (VOI) using automated features within the commercial software mentioned earlier.

The SUV_{max} for the spleen (SUV_{spleen}) were measured by manual placing of spherical VOI at the center of the spleen, corresponding to the largest anterior-posterior diameter observed in the axial image²⁸. To validate the method of spleen SUV measurement, inter-rater variability was assessed.

The assessment of VAT metabolic activity using FDG PET starts by identifying VAT regions on CT images, defined by Hounsfield units ranging from −110 to −70HU, corresponding to human adipose tissue density¹³. A multi-slice approach is employed for Region of Interest (ROI) placement, selecting three consecutive slices in the abdominal VAT area and placing two-dimensional ROIs on each. Accuracy is ensured by carefully adjusting ROI placement to exclude non-VAT uptake, achieved through simultaneous review of PET and CT slices. This process minimizes potential spillover effects from neighboring tissues, such as physiological FDG uptake in the bowel. The SUV_{max} is calculated for each ROI, and an average SUV across the multiple ROIs is determined, providing a representative measure of SUV_{VAT}.

Statistical analysis

Basic statistical analyses were performed using two commercial software programs (version 26.0, IBM SPSS Statistics, Armonk, NY, USA; Rex 3.6.0, Rexsoft, Seoul, Korea). All statistical tests were 2-sided with a significance threshold of $P < 0.05$.

The Kaplan-Meier survival curve was generated to estimate cumulative DFS rates. All continuous variables in survival analysis were dichotomized by specific cutoff values, which were resulted by the receiver operating characteristic (ROC) analysis. Survival curves were compared with the log-rank test. To determine whether the combination of independent parameters have the potential to predict recurrence, ROC curve and the area under the ROC curve (AUC) were calculated. Multivariable logistic regression models based on parameters with significant group differences were built in a stepwise manner to combine different types of markers. The ROC curves were compared with Bootstrap method.

Data availability

Raw sequence reads analyzed in the present study are available at the National Center for Biotechnology Information (NCBI) Sequence Read Archive (SRA) under BioProject ID PRJNA1179894.

Received: 14 October 2024; Accepted: 26 February 2025

Published online: 10 March 2025

References

1. Arnold, M. et al. Current and future burden of breast cancer: global statistics for 2020 and 2040. *Breast* **66**, 15–23 (2022).
2. Zhou, M. et al. Discovery of potential prognostic long non-coding RNA biomarkers for predicting the risk of tumor recurrence of breast cancer patients. *Sci. Rep.* **6**, 31038 (2016).
3. Duffy, M. J. Serum tumor markers in breast cancer: are they of clinical value? *Clin. Chem.* **52**, 345–351 (2006).

4. Sheng, A., Zhang, H., Li, Q., Chen, S. & Wang, Q. Application of intelligent response fluorescent probe in breast Cancer. *Molecules* **29**, 4294 (2024).
5. Sadrekarimi, H. et al. Emerging role of human Microbiome in cancer development and response to therapy: special focus on intestinal microflora. *J. Translational Med.* **20**, 301 (2022).
6. Ağagündüz, D. et al. Understanding the role of the gut Microbiome in Gastrointestinal cancer: A review. *Front. Pharmacol.* **14**, 1130562 (2023).
7. Hong, W. et al. Gut Microbiome causal impacts on the prognosis of breast cancer: a Mendelian randomization study. *BMC Genom.* **24**, 497 (2023).
8. Sampsell, K., Hao, D. & Reimer, R. A. The gut microbiota: a potential gateway to improved health outcomes in breast cancer treatment and survivorship. *Int. J. Mol. Sci.* **21**, 9239 (2020).
9. Fukui, H. Increased intestinal permeability and decreased barrier function: does it really influence the risk of inflammation? *Inflamm. Intestinal Dis.* **1**, 135–145 (2016).
10. Rose, D. P. & Vona-Davis, L. Biochemical and molecular mechanisms for the association between obesity, chronic inflammation, and breast cancer. *Biofactors* **40**, 1–12. <https://doi.org/10.1002/biof.1109> (2014).
11. Lee, M. I. et al. Prognostic value of SUVmax in breast cancer and comparative analyses of molecular subtypes: A systematic review and meta-analysis. *Med. (Baltim.)* **100**, e26745. <https://doi.org/10.1097/md.00000000000026745> (2021).
12. Bang, J. I., Yoon, H. J. & Kim, B. S. Clinical utility of FDG uptake within reticuloendothelial system on F-18 FDG PET/CT for prediction of tumor recurrence in breast cancer. *PLoS One* **13**, e0208861 (2018).
13. Kim, H. J. et al. F-FDG uptake of visceral adipose tissue on preoperative PET/CT as a predictive marker for breast cancer recurrence. *Sci. Rep.* **12**, 18, 21109 (2022).
14. Pahk, K., Joung, C. & Kim, S. Visceral fat metabolic activity evaluated by preoperative 18F-FDG PET/CT significantly affects axillary lymph node metastasis in postmenopausal luminal breast cancer. *Sci. Rep.* **10**, 1348 (2020).
15. Choi, J. E. et al. Breast cancer statistics in Korea, 2019. *J. Breast Cancer* **26**, 207 (2023).
16. Precup, G. & Vodnar, D. C. Gut Prevotella as a possible biomarker of diet and its eubiotic versus dysbiotic roles: a comprehensive literature review. *Br. J. Nutr.* **122**, 131–140 (2019).
17. Ou, J. et al. Diet, microbiota, and microbial metabolites in colon cancer risk in rural Africans and African Americans. *Am. J. Clin. Nutr.* **98**, 111–120 (2013).
18. Huh, J. W. et al. Enterotypical Prevotella and three novel bacterial biomarkers in preoperative stool predict the clinical outcome of colorectal cancer. *Microbiome* **10**, 203 (2022).
19. Larsen, J. M. The immune response to Prevotella bacteria in chronic inflammatory disease. *Immunology* **151**, 363–374 (2017).
20. Bouras, E. et al. Circulating inflammatory cytokines and risk of five cancers: a Mendelian randomization analysis. *BMC Med.* **20**, 1–15 (2022).
21. il Lee, M. et al. Prognostic value of SUVmax in breast cancer and comparative analyses of molecular subtypes: a systematic review and meta-analysis. *Medicine* **100**, e26745 (2021).
22. Yoon, H. J. et al. Physiologic intestinal 18F-FDG uptake is associated with alteration of gut microbiota and Proinflammatory cytokine levels in breast cancer. *Sci. Rep.* **9**, 18273 (2019).
23. Kozich, J. J., Westcott, S. L., Baxter, N. T., Highlander, S. K. & Schloss, P. D. Development of a dual-index sequencing strategy and curation pipeline for analyzing amplicon sequence data on the miseq illumina sequencing platform. *Appl. Environ. Microbiol.* **79**, 5112–5120 (2013).
24. Fadrosch, D. W. et al. An improved dual-indexing approach for multiplexed 16S rRNA gene sequencing on the illumina miseq platform. *Microbiome* **2**, 1–7 (2014).
25. Yoon, S. H. et al. Introducing EzBioCloud: a taxonomically united database of 16S rRNA gene sequences and whole-genome assemblies. *Int. J. Syst. Evol. Microbiol.* **67**, 1613–1617 (2017).
26. Nguyen, N. P., Warnow, T., Pop, M. & White, B. A perspective on 16S rRNA operational taxonomic unit clustering using sequence similarity. *NPJ Biofilms Microbiomes* **2**, 16004. <https://doi.org/10.1038/npjbiofilms.2016.4> (2016).
27. Segata, N. et al. Metagenomic biomarker discovery and explanation. *Genome Biol.* **12**, 1–18 (2011).
28. Yoon, H. J. et al. Prognostic value of diffuse Splenic FDG uptake on PET/CT in patients with gastric cancer. *PLoS One* **13**, e0196110 (2018).

Acknowledgements

This work was supported by the National Research Foundation of Korea (NRF) grant funded by the Korea government (MSIT) (RS-2024-00453521, RS-2024-00449684, RS-2024-00439928, RS-2022-NR067387, and RS-2021-NR058775), the Ministry of Health and Welfare (RS-2023-00262969), and the grants of the Korean Association for Women Surgeons (202201770001).

Author contributions

H.Y. supervised this study. H.Y. and B.K. collected the data. J.A. and H.Y. conducted the analyses and interpreted the data. J.A. and H.Y. drafted the manuscript. J.A., H.Y. and B.K. critically revised the manuscript.

Declarations

Competing interests

The authors declare no competing interests.

Additional information

Supplementary Information The online version contains supplementary material available at <https://doi.org/10.1038/s41598-025-92233-z>.

Correspondence and requests for materials should be addressed to B.S.K. or H.-J.Y.

Reprints and permissions information is available at www.nature.com/reprints.

Publisher's note Springer Nature remains neutral with regard to jurisdictional claims in published maps and institutional affiliations.

Open Access This article is licensed under a Creative Commons Attribution-NonCommercial-NoDerivatives 4.0 International License, which permits any non-commercial use, sharing, distribution and reproduction in any medium or format, as long as you give appropriate credit to the original author(s) and the source, provide a link to the Creative Commons licence, and indicate if you modified the licensed material. You do not have permission under this licence to share adapted material derived from this article or parts of it. The images or other third party material in this article are included in the article's Creative Commons licence, unless indicated otherwise in a credit line to the material. If material is not included in the article's Creative Commons licence and your intended use is not permitted by statutory regulation or exceeds the permitted use, you will need to obtain permission directly from the copyright holder. To view a copy of this licence, visit <http://creativecommons.org/licenses/by-nc-nd/4.0/>.

© The Author(s) 2025